Chinese Chemical Letters 34 (2023) 107672

Contents lists available at ScienceDirect

Chinese Chemical Letters

journal homepage: www.elsevier.com/locate/cclet

Fluorescence immunoassay based on alkaline phosphatase-induced *in situ* generation of fluorescent non-conjugated polymer dots

Donghui Wu[a,b], Qilin Zhao[a,b], Jian Sun[a,*], Xiurong Yang[a,b,*]

[a] State Key Laboratory of Electroanalytical Chemistry, Changchun Institute of Applied Chemistry, Chinese Academy of Sciences, Changchun 130022, China
[b] School of Applied of Chemistry and Engineering, University of Science and Technology of China, Hefei 230026, China

ARTICLE INFO

Article history:
Received 7 April 2022
Revised 22 June 2022
Accepted 8 July 2022
Available online 9 July 2022

Keywords:
Alkaline phosphatase
Non-conjugated polymer dots
Fluorescent sensor
Fluorescent ELISA
Cardiac troponin I

ABSTRACT

Alkaline phosphatase (ALP) activity assay is not only significant to the clinical diagnosis of some related disease, but also momentous to the construction of ALP-based enzyme-linked immunosorbent assay (ELISA). Herein, for the first time, we have discovered that ascorbic acid (AA) can specially react with *N*-methylethylenediamine (N-MEDA) to generate fluorescent non-conjugated polymer dots (NCPDs) under mild conditions. On the basis of the AA-responsive emission and ALP-catalyzed hydrolysis of ascorbic acid 2-phosphate (AA2P) to AA, we have exploited a fluorometric ALP activity assay with high sensitivity and selectivity. Furthermore, by means of conventional ALP-based ELISA platform, a conceptual fluorescent ELISA has been constructed and applied in the potential clinical diagnosis, during which cardiac troponin I (cTnI), a well-established biomarker of acute myocardial infarction, has been chosen as the model target. We envision that such original fluorescent NCPDs generation-enabled ELISA could become a versatile tool in biochemical sensing and medical diagnosis in the future.

Alkaline phosphatase (ALP), a crucial hydrolytic enzyme in phosphate metabolism, in charge of the dephosphorylation process of proteins, nucleic acids, or small molecules in living organisms. Abnormal levels of ALP in human serum can lead to many diseases including osteopathy, hepatobiliary diseases, breast and prostatic cancer, diabetes and Alzheimer's disease [1,2]. Furthermore, ALP has been broadly used for enzyme-linked immunosorbent assay (ELISA) as a labeled enzyme owing to its merits of high catalytic activity and good stability [3]. Profiting just from such excellent properties of labeled enzyme as well as the specificity of antigen-antibody binding, ELISA has been considered as the gold standard for detection and quantification of specific biomarkers in the disease diagnosis, food safety testing, and environmental monitoring [4]. Therefore, the establishment of reliable methods for the sensitive detection of ALP activity is of great significance for both the ALP-related diseases diagnosis and ALP-based ELISA platforms.

By means of the ability to remove phosphate groups from various kinds of phosphate substates, a lot of analytical methods including colorimetric, fluorometric, chemiluminescence and electrochemical approaches have been established for ALP assay [5–8]. Among these assays, fluorescence method, especially the nanomaterial-based fluorescence assay, has been highlighted due to the rapid response, low cost, and the superior properties of nanomaterials, which can conspicuously improve the detection sensitivity and performances [9–12]. Various fluorescent nanomaterial such as metal nanoclusters (NCs) [13–15], quantum dot [16,17], and coordination polymers [18] have become the attractive candidate for fluorescent probes due to their incomparable advantages. However, most of the current nanomaterial-based fluorescence strategies for ALP detection directly evaluate the fluorescence variations of as-prepared nanomaterials, during which several transition metal ions (Cu^{2+}, Fe^{3+} and so on), and/or phosphate-containing molecules have been used as intermediates [19–22]. Generally, such strategy not only involved sophisticated synthetic, modification and purification processes of the fluorescent nanomaterials but also accompanied with strong background signals and relatively low sensitivity [23–25]. On the contrary, instead of using the quenching capability of the ALP-resulting product nor synthesizing the nanoprobe in advance, designing a "turn-on" strategy based on enzyme-induced *in situ* formation of fluorescent nanomaterials can greatly simplify the entire detection process and improve the sensitivity of the system.

As an emerging class of fluorescent nanomaterials, the non-conjugated polymer dots (NCPDs), which is only in possession of heteroatom-containing double bonds and single bonds subfluorophores, such as C=O, C=N, N=O, C–O and amino-based groups, have sparked intense research interest with its prominent photoluminescence, great stability, and low toxicity [26,27]. Differ-

* Corresponding authors.
E-mail addresses: jiansun@ciac.ac.cn (J. Sun), xryang@ciac.ac.cn (X. Yang).

https://doi.org/10.1016/j.cclet.2022.07.015
1001-8417/

ent from conjugated polymer dots, the NCPDs is always prepared from non-conjugated polymers or small molecules by condensation and crosslinking routes instead of constructed by the assembly of conjugated polymers and are therefore more water-soluble, extending their applications in bio-related fields such as drug delivery, biosensing, and bioimaging [27–30]. Although lacking conjugated structures, the fluorescence of these sub-fluorophores can be enhanced by chemical crosslinking or physical immobilization of polymer chains. This is called the crosslink-enhanced emission (CEE) effect [31]. Despite many advances and endeavors, most of the current generation of NCPDs relies on the hydrothermal and microwave method at high temperature and/or high pressure, which usually involves external energy input [26].

Herein, we have developed a facile fabrication strategy towards the one-step synthesis of fluorescent NCPDs based on *N*-methylethylenediamine (N-MEDA) and ascorbic acid (AA) under mild conditions for the first time. More impressively, we have further confirmed that the fluorescence reaction is very specific and almost cannot be realized if using the phosphate substrate ascorbic acid 2-phosphate (AA2P) instead of AA, which inspired us to design and develop a convenient fluorescent method for assaying ALP activity. Furthermore, utilizing the commonly used ALP-labeled immunoassay platform and corresponding antibodies, we have constructed a novel NCPDs-based fluorescent ELISA by using cardiac troponin I (cTnI), a serologic marker for the early diagnosis of acute myocardial infarction (AMI) as a model antigen. In our fluorescent ELISA, the level of cTnI is directly connected with the level of ALP-labeled secondary antibody and can be indirectly acquired *via* determining the fluorescence intensities of the resultant NCPDs solution. In fact, such mild reaction between AA and N-MEDA results in intense fluorescence appearing from scratch, bestowing both the ALP activity assay and ALP-based ELISA excellent sensing performance and potential application in clinical diagnosis.

Firstly, using two non-conjugated small molecules AA and N-MEDA as precursors, we put forward a more convenient and mild synthetic strategy for fluorescent NCPDs. As presented in Fig. 1A, without any external energy supply, just simply mixing the solution of N-MEDA and AA at room temperature can obtain the water-soluble fluorescent NCPDs with colorless and transparent under sunlight. The as-prepared NCPDs solution has blue emission (inset in Fig. 1B), which is because the fluorescence of NCPDs is mainly controlled by the immobilized sub-fluorophore and thus has a very wide band gap [32]. In addition, it exhibits obvious absorption band around 300–350 nm and has a maximum emission wavelength around 425 nm with the excitation wavelength around 350 nm, which is consistent well with its absorption spectrum (Fig. 1B). The quantum yield (QY) of the NCPDs is calculated to be 2.8% by use of quinine sulfate as a standard (QY = 54%, Fig. S1 in Supporting information). We also examined the fluorescence lifetime by time-correlated single photon counting (TSCPC) at 350 nm excitation and the resultant average lifetime is 2.7 ns (Fig. S2 in Supporting information). It is noteworthy that the emission wavelength of the as-prepared fluorescent NCPDs exhibits a bathochromic shift when the excitation wavelength increases from 300 nm to 380 nm (Fig. S3 in Supporting information). Such excitation-dependent emission behavior is due to the fact that each NCPD nanoparticle is composed of a large number of sub-fluorophore and every sub-fluorophore may be in different chemical environments, so there various photoluminescence (PL) states may exist in the NCPDs [25]. For the subsequent application in ALP sensing, we verified the stability of as-prepared NCPDs. As exhibited in Fig. S4 (Supporting information), after 60 min of UV irradiation (350 nm), the NCPDs displayed an extraordinary photostability. Moreover, the fluorescence is insensitive to ionic strength, indicates that NCPDs are highly stable and will be conducive to their potential biological applications. The TEM image can be used to reveal the morphology and directly confirm the formation of fluorescent NCPDs. As depicted in Fig. 1C, the as-obtained NCPDs exhibit a dot-shape with diameters of 14–49 nm.

Furthermore, the FT-IR and XPS were collected to investigate the surface compositions of the fluorescent NCPDs. As shown in Fig. 1D, compared with the precursors AA and N-MEDA, the FT-IR spectrum of the NCPDs exhibits several distinct characteristic functional groups at 1600–1670 cm^{-1}, which is assigned to the stretching vibration of amide linkage and/or C=N [33,34]. This result suggests that AA may react with N-MEDA by the reversible amide and/or Schiff base reaction. To prove this, $NaBH_4$, the commonly used reducing agent that can reduce C=N to C–N [32,35], was introduced to the reaction system. As depicted in Fig. S5 (Supporting information), the fluorescence intensities were significantly decreased after adding the $NaBH_4$ to the mixture solution of AA and N-MEDA, during which the existence of Schiff base reaction was proved. Moreover, the broad absorption band between 3500 cm^{-1} and 2900 cm^{-1} indicates that the functional groups –NH and –OH

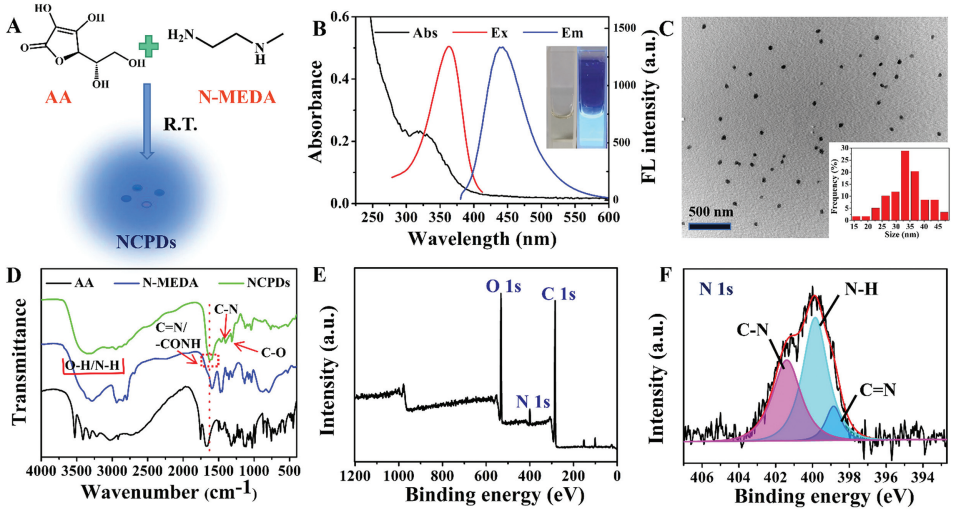

Fig. 1. (A) Schematic illustration of one-step synthesis of NCPDs based on AA and N-MEDA. (B) Absorption, fluorescence excitation and emission spectra of NCPDs. The inset shows the corresponding colors of the NCPDs solutions under a daylight (left) and 365 nm UV lamp (right). (C) TEM image of NCPDs. Inset is the size distribution of NCPDs. (D) FT-IR spectra of AA, N-MEDA and NCPDs. (E) The full survey of the XPS spectrum of NCPDs. (F) The high-resolution XPS spectrum of N 1s.

are interconnected by a hydrogen bond [36]. The stretching vibrations of other functional groups in fluorescent NCPDs, such as C–O and C–N can be also observed at 1402 cm^{-1} and 1314 cm^{-1}, respectively [37]. As shown in Fig. 1E, the full XPS spectrum of the fluorescent NCPDs have three typical peaks at 284.5 eV, 400.4 eV and 531.8 eV, respectively, indicating that the nanoparticles mainly consisted of C, N, O elements [38]. The N 1s spectrum (Fig. 1F) contains three peaks at 398.8 eV, 399.8 eV and 401.4 eV, which be assigned to C=N, N–H, and C–N bonds, respectively [8]. Meanwhile, the presence of C=N bond also certifies the occurrence of Schiff base reaction. The high-resolution C 1s spectrum (Fig. S6A in Supporting information) can be divided into three peaks at 284.5 eV, 285.7 eV and 288.5 eV, which belong to C=C/C–C, C–N/C–O and C=N/C=O. The O 1s spectrum (Fig. S6B in Supporting information) can be deconvoluted into two peaks located at 531.8eV and 532.8eV, corresponding to C=O and C-O bond [39]. The FT-IR data is in good agreement with the XPS analysis, where these abundant functional groups on the surface of NCPDs also endow the NCPDs with good aqueous dispersibility [40]. Combined with the above results and previous reports, we speculated the possible formation mechanism of the as-prepared NCPDs are as follows. Firstly, AA is readily oxidized to radical monodehydroascorbate (MDHA) under the alkaline aqueous condition, then converts into unstable dehydroascorbate (DHA) and ultimately turns into 2,3-diketogulonic acid *via* irreversible hydrolytic ring cleavage in aqueous medium [41]. Subsequently, these abundant molecular species, concluding AA, MDHA, DHA, 2,3-diketogulonic acid and N-MEDA, undergo dehydration and condensation *via* amide and Schiff base reactions [42], and further cross-linked by supramolecular interactions such as hydrogen bonding and van der Waals interactions to form NCPDs [43]. In this process, the sub-fluorophores such as –NH, –OH, C=O, C=N are immobilized, reducing non-radiative transitions and enhancing fluorescence based on the apparent CEE effect.

Considering that AA, the necessary reagent for NCPDs synthesis, can be obtained by ALP-catalyzed dephosphorylation of AA2P, the synthesis process provides a possibility to realize the determination of ALP activity. As shown in Figs. 2A and B, when the concentration of N-MEDA remains constant, the fluorescence intensities of the fluorescent NCPDs solution gradually enhanced with the increasing concentration of AA and exhibit a good liner relationship ($R^2 = 0.999$). Therefore, such concentration dependence encouraged

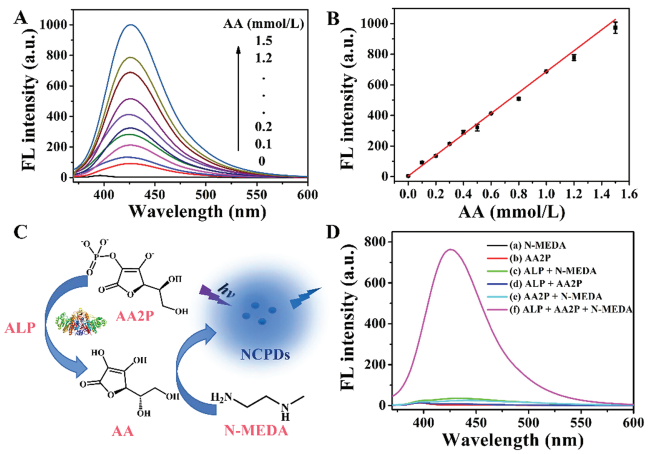

Fig. 2. (A) Fluorescence emission spectra and (B) corresponding fluorescence intensities of N-MEDA (50 mmol/L) in addition of different concentrations of AA (0-1.5 mmol/L). pH 9.8 (50 mmol/L DEA). (C) Principle of ALP-induced generation of NCPDs. (D) FL emission spectra of (a) N-MEDA, (b) AA2P (c) ALP + N-MEDA, (d) ALP + AA2P, (e) AA2P + N-MEDA, (f) ALP + AA2P + N-MEDA. The concentrations of ALP, AA2P and N-MEDA are 60 mU/mL, 3 mmol/L and 50 mmol/L, respectively.

us to develop a fluorescent sensing strategy for ALP assay by using AA2P as the substrate and AA as a transducer component of the NCPDs (Fig. 2C). On the basis of the fact that ALP shows optimal activity at a working pH of 9.8 [44], the diethanolamine buffer (DEA, pH 9.8), a commonly used alkaline buffer in the enzymatic assay of ALP was selected. Fortunately, the DEA molecule never hampers the generation of fluorescent NCPDs owing to its favorable chemical stability and biocompatibility [45].

Next, several control tests were implemented to verify the feasibility of the ALP sensing strategy. As shown in Fig. 2D, both of the sole N-MEDA (curve a) and AA2P (curve b) solution have no apparent fluorescence signal and the addition of ALP (curve c and d) can hardly induce any obvious change. As expected, only when ALP, AA2P and N-MEDA (curve f) exist at the same time, a substantially enhanced fluorescence readout could be observed. However, it is worth noting that the mixture of AA2P and N-MEDA (curve e) could produce very weak signals in the absence of ALP. We speculate that it may be due to the following reasons. Firstly, compared with AA, AA2P is much more stable in aqueous solution, and is not easily oxidized into unstable dehydrogenation intermediates and a series of subsequent substances, so it has fewer reaction sites. Moreover, the steric-hinderance effect resulting from the phosphate group of AA2P also hinders the crosslinking with N-MEDA. As mentioned above, by means of the ability of N-MEDA to distinguish AA and AA2P, a new fluorescent "turn-on" strategy for monitoring ALP activity by enzyme-triggered *in situ* formation of fluorescent NCPDs could be proposed.

In order to obtain a preferable performance of our proposed assay, the concentration of reactant and other experimental conditions have been explored and optimized in detail. Generally, the concentration of the substrate is closely related to the detection range and sensitivity of the enzyme assay, therefore, the concentrations of AA2P and N-MEDA were evaluated first and optimized at 3 mmol/L and 50 mmol/L (Fig. S7 in Supporting information), respectively. In addition, the other experimental conditions such as pH, fluorogenic reaction temperature, enzymatic and fluorogenic reaction time were also investigated and finally optimized to 9.8, 70 °C, 60 min and 120 min, respectively (Fig. S8 in Supporting information).

Under the aforesaid optimized experiment conditions, the sensing performance of this fluorometric ALP activity assay was evaluated. As illustrated in Fig. 3A, the gradual enhancement in fluorescence intensity is exhibited with the increased activity of ALP. In particular, as the activity of ALP changed from 0 to 150 mU/mL, a two-stage good linear relationship was displayed (Figs. 3B and C). The fitted linear data of the fluorescence readout could be expressed as $F_1 = 42.50 + 18.47\ C_{ALP}$ ($R^2 = 0.997$) and $F_2 = 184.33 + 9.60\ C_{ALP}$ ($R^2 = 0.998$), respectively. The limit of detection (LOD) of our fluorescent assay is 0.12 mU/mL, which displayed a better analytical performance in ALP activity determination in comparison with other previously reported ALP assays (Table S1 in Supporting information). Moreover, to verify the dependability of our designed fluorescent sensor for ALP, several common biomolecules, including bovine serum albumin (BSA), glucose oxidase (Gox), horseradish peroxidase (HRP), lysozyme (LZM), trypsin, tyrosinase, and acetyl cholinesterase (AchE) were selected as the potential interfering substances. As described in Fig. 3D, none of them can bring apparent fluorescence impact in the NCPDs formation-based sensing system and interfere in the recognition response of ALP. This result manifests that our approach exhibited the excellent selectivity for sensing ALP activity.

Subsequently, the practical feasibility of our proposed strategy in complex biological samples was investigated *via* measuring ALP activity in the diluted normal human serum (1%). The result in Table S2 (Supporting information) exhibits an excellent recovery in the range of 106.4%-111.9% with the relative standard

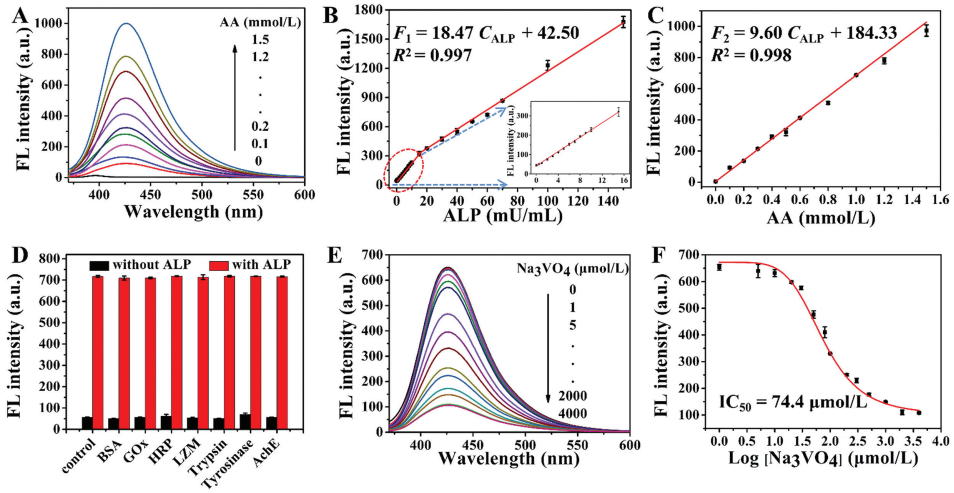

Fig. 3. (A) Fluorescence emission spectra at different ALP concentrations excited at 350 nm. (B, C) Linear range of fluorescence intensities against concentrations of ALP from 0 to 150 mU/mL. (D) Selectivity investigation of the proposed sensing system for ALP activity (60 mU/mL). The concentrations of interfering proteins were 10 μg/mL, respectively. (E) Fluorescence spectra of the ALP assay with different concentrations of Na_3VO_4. (F) Sigmoidal fitting of the fluorescence intensity *versus* the logarithm of Na_3VO_4 concentrations.

deviation (RSD) less than 5%, reflecting that our sensing system can be used to determine ALP activity in practical applications. Moreover, the screening of enzyme inhibitors is of great significance for drug design and discovery. Na_3VO_4, a well-known inhibitor for ALP, which can not affect the fluorogenic reaction between AA and N-MEDA (Fig. S9 in Supporting information) was adopted to assess the inhibition efficiency of ALP activity. As depicted in the Figs. 3E and F, the fluorescence intensities of our sensing system exhibited a concentration-dependent decrease with the concentrations of Na_3VO_4 increasing from 0 to 4000 μmol/L, and obtained a typical S-curve between fluorescence intensities and the logarithms of the Na_3VO_4 concentrations. The half-maximal inhibitory concentration (IC_{50}) of Na_3VO_4 is approximately 74.4 μmol/L, which was in accordance with those of the previous ALP inhibitor screening [7].

Cardiac troponin I (cTnI), a specialized cardiac regulatory protein, is recognized as the gold standard for the early diagnosis of acute myocardial infarction (AMI). In fact, the detection of cTnI can play an important role in the diagnosis of cardiovascular disease [46]. By means of the widespread use of ALP as a labeling enzyme in ELISA and available commercial cTnI antibodies, we attempted to extend our ALP-induced fluorogenic reaction into an ELISA template for the cTnI determination (Fig. 4A). Following the routine co-immobilization of capture antibody (Capture Ab), cTnI standards with different concentrations, anti-cTnI antibody (Ab1), and ALP-labeled secondary antibody (ALP-Ab2) onto a 96-well plate, AA2P were added to produce AA. Subsequently, N-MEDA was added to generate the NCPDs and give a fluorescence signal. In this respect, a higher cTnI concentration results in more ALP-Ab2 being captured on the 96-well plate, thereby producing a stronger fluorescence readout signal. As disclosed in Figs. 4B and C, the fluorescence intensity shows a cTnI concentration-dependent enhancement. The relationship between fluorescence intensities and cTnI concentrations (0-100 ng/mL) can be described as $F = 33.9 + 1.87\ C_{cTnI}$ (ng/mL), $R^2 = 0.996$. The evaluated detection limit of the proposed strategy is 0.4 ng/mL according to the 3σ rule, which is superior to that of the previous reports for cTnI detection (Table S3 in Supporting information).

High specificity is an important indicator to verify the potential of our designed ALP-enabled ELISA in complex biological samples. Therefore, several non-specific proteins and enzymes, which include cardiac troponin T (cTnT), alpha fetoprotein (AFP), immunoglobulin G (IgG), LZM, AchE, and carcinoembryonic antigen

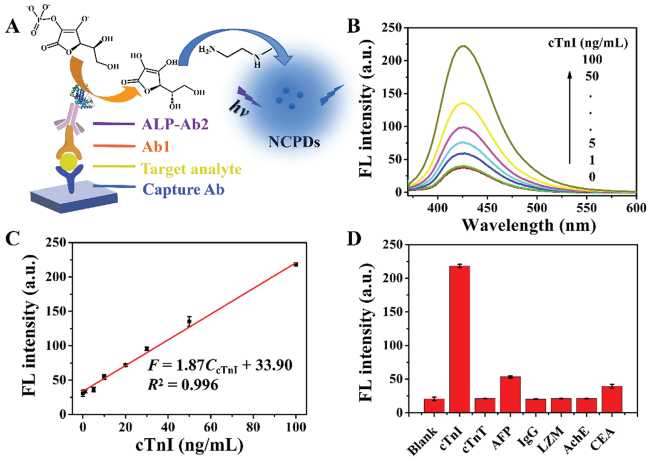

Fig. 4. (A) Schematic presentation of the fluorescent ELISA. (B) The fluorescence emission spectra and (C) the corresponding fluorescence intensities at 425 nm of the fluorescent ELISA as a function of cTnI activities (0-100 ng/mL). (D) Selectivity investigation of the proposed fluorescent ELISA against cTnI or other interfering proteins (100 ng/mL).

(CEA) were introduced as potential competitors. As shown in Fig. 4D, neither of them can bring about marked changes in the fluorescence signals, and only cTnI can arouse an intense fluorescence response owing to the specific antigen-antibody recognition. These results unequivocally imply that our fluorescent ELISA shows excellent specificity for cTnI detection. Of greater significance, the feasibility of our proposed fluorescent ELISA for analysis in actual serum samples was investigated by evaluating the diluted normal human serum (1%) containing various concentrations of cTnI, and the fluorescence response results are compared with commercial pNPP-based ELISA kits for cTnI. Table S4 (Supporting information) depicted that the results of the conventional colorimetric ELISA are consistent with that of as-proposed fluorescent ELISA, which verifies that our fluorescent ELISA possesses great prospects in the clinical diagnosis of disease biomarkers with excellent performance.

In conclusion, we have developed a facile one-step approach for the synthesis of fluorescent NCPDs using AA and N-MEDA as the precursors for the first time. Moreover, inspired by the fact

that AA can be produced *via* ALP-catalyzed dephosphorylation of AA2P and the specific fluorescence reaction between AA and N-MEDA, a definite fluorescent sensor for ALP activity assay and ALP inhibitor screening has been successfully established. More significantly, utilizing the explicit recognition mechanism and excellent sensing performance, we further constructed a novel fluorescent ELISA by ALP-mediated *in situ* formations of fluorescent NCPDs for the sensitive measurement of model antigen. In addition, our proposed assay could be successfully employed to evaluate the cTnI concentration in serums, which meets the requirements of potential clinical diagnosis of AMI and coincides with those of standard colorimetric ELISA. We believe that our suggested ALP activity assay based on the fluorescent "turn-on" strategy and corresponding ELISA platform will obtain high practicality and superiority in both laboratory research and clinical diagnosis in the near future.

Declaration of competing interest

The authors declare that they have no known competing financial interests or personal relationships that could have appeared to influence the work reported in this paper.

Acknowledgments

We thank the financial supports of theNational Natural Science Foundation of China (Nos. 22034006, 21974132 and 21721003), the Youth Innovation Promotion Association, CAS (No. 2018258), and the Development Project of Science and Technology of Jilin Province, China (No. 20200201091JC).

Supplementary materials

Supplementary material associated with this article can be found, in the online version, at doi:10.1016/j.cclet.2022.07.015.

References

[1] C. Chen, D. Zhao, B. Wang, et al., Anal. Chem. 92 (2020) 4639–4646.
[2] L. Dong, Q.Q. Miao, Z.J. Hai, Y. Yuan, G.L. Liang, Anal. Chem. 87 (2015) 6475–6478.
[3] L. Wu, G.H. Li, X. Xu, et al., TrAC-Trend. Anal. Chem. 113 (2019) 140–156.
[4] L. Gao, Q. Yang, P. Wu, F. Li, Analyst 145 (2020) 4069–4078.
[5] D. Zhao, J. Li, C. Peng, et al., Anal. Chem. 91 (2019) 2978–2984.
[6] J. Sun, T. Hu, C. Chen, et al., Anal. Chem. 88 (2016) 9789–9795.
[7] J.H. Zhao, S. Wang, S.S. Lu, et al., Anal. Chem. 91 (2019) 7828–7834.
[8] G.Y. Liu, J.H. Zhao, M.X. Yan, et al., Sci. China Chem. 63 (2020) 554–560.
[9] T Balbaied, E Moore, Biosensors 9 (2019) 102.
[10] F.S. Niu, Y.L. Ying, X. Hua, et al., Carbon 127 (2018) 340–348.
[11] D. Zhao, X. Ma, N. Li, et al., Chin. J. Anal. Chem. 49 (2021) 1804–1815.
[12] H.Y. Zhang, Q.K. Ju, S.D. Pang, et al., Dyes Pigments 194 (2021) 109569.
[13] M.C. Pan, Y.M. Lei, Y.Q. Chai, R. Yuan, Y. Zhuo, Anal. Chem. 92 (2020) 13581–13587.
[14] X.L. Hu, X.M. Wu, X. Fang, Z.J. Li, G.L. Wang, Biosens. Bioelectron. 77 (2016) 666–672.
[15] K.Y. Huang, H.X. He, S.B. He, et al., Sens. Actuators B: Chem. 296 (2019) 126656.
[16] J.J. Liu, D.S. Tang, Z.T. Chen, et al., Biosens. Bioelectron. 94 (2017) 271–277.
[17] Z.S. Qian, L.J. Chai, C. Tang, et al., Anal. Chem. 87 (2015) 2966–2973.
[18] J.J. Deng, P. Yu, Y.X. Wang, L.Q. Mao, Anal. Chem. 87 (2015) 3080–3086.
[19] S.G. Liu, L. Han, N. Li, et al., J. Mater. Chem. B. 6 (2018) 2843–2850.
[20] M.I. Kim, S.Y. Park, K.S. Park, et al., Sens. Actuators B: Chem. 262 (2018) 469–476.
[21] G.L. Li, H.L. Fu, X.J. Chen, et al., Anal. Chem. 88 (2016) 2720–2726.
[22] J.Z. Liu, H.M. Meng, L. Zhang, et al., Chin. Chem. Lett. 32 (2021) 3421–3425.
[23] Y.X. Han, J. Chen, Z. Li, H.L. Chen, H.D. Qiu, Biosens. Bioelectron. 148 (2020) 111811.
[24] M. Li, B. Gurram, S. Lei, et al., Chin. Chem. Lett. 32 (2021) 1316–1330.
[25] Z.W. Tang, H.T. Chen, H.L. He, C.B. Ma, TrAC-Trend. Anal. Chem. 113 (2019) 32–43.
[26] S.J. Zhu, Y.B. Song, J.R. Shao, X.H. Zhao, B. Yang, Angew. Chem. Int. Ed. 54 (2015) 14626–14637.
[27] S.J. Zhu, L. Wang, N. Zhou, et al., Chem. Commun. 50 (2014) 13845–13848.
[28] Y. Sun, W. Cao, S. Li, et al., Sci. Rep. 3 (2013) 3036.
[29] J.S. Liu, H.J. Bao, C.F. Liu, F.F. Wu, F. Gao, ACS Appl, Polym. Mater. 1 (2019) 3057–3063.
[30] Y. Fan, J. Yao, M.K. Huang, et al., Food Chem. 359 (2021) 129962.
[31] S.Y. Tao, S.J. Zhu, T.L. Feng, C.Y. Zheng, B. Yang, Angew. Chem. Int. Ed. 59 (2020) 9826–9840.
[32] N. Orlova, I. Nikolajeva, A. Pučkins, S. Belyakov, E. Kirilova, Molecules 26 (2021) 2570.
[33] J. Xia, S. Chen, G.Y. Zou, Y.L. Yu, J.H. Wang, Nanoscale 10 (2018) 22484–22492.
[34] J. Xia, Y.T. Zhuang, Y.L. Yu, J.H. Wang, Microchimica Acta 184 (2017) 1109–1116.
[35] P. Yang, X. Zhou, J. Zhang, et al., Green Chem. 23 (2021) 1834–1839.
[36] T. Edison, R. Atchudan, M.G. Sethuraman, J.J. Shim, Y.R. Lee, J. Photochem. Photobiol. B. 161 (2016) 154–161.
[37] L. Vallan, E.P. Urriolabeitia, F. Ruiperez, et al., J. Am. Chem. Soc. 140 (2018) 12862–12869.
[38] Z. Zhou, P. Tian, X. Liu, Adv. Sci. 5 (2018) 1800369.
[39] S. Lu, L. Sui, J. Liu, et al., Adv. Mater. 29 (2017) 1603443.
[40] A. Jana, Y.J. Lee, J.S. Chung, M.H. Kim, S.Y. Hur, Anal. Chim. Acta 1079 (2019) 212–219.
[41] M.W. Davey, M. Van Montagu, D. Inze, et al., J. Sci. Food Agric. 80 (2000) 825–860.
[42] Z.F. Huang, X.Q. Zhang, X.Y. Zhang, et al., Polym. Chem. 6 (2015) 2133–2138.
[43] S. Mavila, O. Eivgi, I. Berkovich, N.G. Lemcoff, Chem. Rev. 116 (2016) 878–961.
[44] Z.G. Song, R.T.K. Kwok, E.G. Zhao, et al., ACS Appl. Mater. Interfaces 6 (2014) 17245–17254.
[45] J. Sun, J.H. Zhao, X.F. Bao, Q.F. Wang, X.R. Yang, Anal. Chem. 90 (2018) 6339–6345.
[46] X. Han, S. Li, Z. Peng, A.M. Othman, R. Leblanc, ACS Sensors 1 (2016) 106–114.